

# A 3-D Non-Stationary Wideband MIMO Channel Model Allowing for Velocity Variations of the Mobile Station

Ji Bian<sup>1</sup>, Cheng-Xiang Wang<sup>2,1</sup>, Minggao Zhang<sup>1</sup>, Xiaohu Ge<sup>3</sup>, and Xiqi Gao<sup>4</sup>

<sup>1</sup> Shandong Provincial Key Lab of Wireless Communication Technologies, Shandong University, Jinan, 250100, China.

<sup>2</sup>Institute of Sensors, Signals and Systems, School of Engineering & Physical Sciences, Heriot-Watt University, Edinburgh, EH14 4AS, UK.

<sup>3</sup> Department of Electronics and Information Engineering, Huazhong University of Science and Technology, Wuhan 430074, Hubei, China.

<sup>4</sup>National Mobile Communications Research Laboratory, Southeast University, Nanjing, 210096, China.

Email: bianjimail@163.com, cheng-xiang.wang@hw.ac.uk, zmg225@163.com, xhge@mail.hust.edu.cn, xqgao@seu.edu.cn

**Abstract**—Most channel models in the literature are based on the assumption that the mobile station (MS) moves along a straight line with a constant speed. In a realistic environment, the MS may experience changes in their speeds and trajectories. In this paper, a three-dimensional (3-D) non-stationary wideband multiple-input multiple-output (MIMO) channel model allowing for velocity variations of the MS is proposed. The parameters are obtained from the WINNER+ channel model to make the simulations more realistic. Statistical properties including spatial cross-correlation function (CCF), temporal autocorrelation function (ACF), and Doppler power spectral density (PSD) are derived and analyzed. Our findings show that a variation of the velocity of the MS has a significant impact on the statistical properties of the channel model. Furthermore, the proposed channel model can be used as a basic framework for future non-stationary channel modeling.

**Index Terms**—Non-stationary, GBSM, statistical properties, trajectory variations, time-variant parameters.

## I. INTRODUCTION

The development of the fifth generation (5G) wireless communication systems is being carried out in full swing [1]–[4]. The mobility features of the 5G wireless communication networks call for the need for accurate and effective channel models which are able to capture the dynamic properties of the real wireless propagation environments. A common assumption in channel modeling is that the channel fulfills the wide-sense stationary (WSS) condition. However, the WSS assumption is only valid when the observation time interval is much shorter than the stationary interval. Channel models with WSS assumption may neglect the non-stationary characteristics of the channel, especially in high mobility scenarios [5]–[7]. In realistic propagation scenarios, the non-stationarity of the channel could be a result of movements of scatterers such as fallen leaves, pedestrians, and vehicles. In [8], a non-stationary 3-D wideband twin-cluster channel model was proposed. The clusters are in motion or stay static with certain probabilities and a birth-death process was adopted to model the clusters' appearance and disappearance. Another major cause leading to wireless channels' non-stationarity is the movement of MS. The COST family channel models, e.g.,

the COST 2100 channel model [9] introduced the concept of visibility region (VR). As the MS enters and leaves different VRs, the active clusters that can be seen by the MS change, resulting in a non-stationary channel.

Most channel models in the literature [10]–[13] are based on the assumption that the MS moves with a constant speed in a fixed direction. However, in a realistic environment, the MS may experience acceleration/deceleration caused by traffic lights and change the movement direction when cornering, which can cause a significant impact on the statistics of wireless channels. However, the channel models allowing for velocity variations of the MS are still very limited. The authors in [14] analyzed the statistics of the channel when the MS moves with a constant acceleration but in a fix direction. The authors in [15] proposed a two-dimensional (2-D) non-stationary channel model allowing the MS to move with varying velocity (both speeds and directions). In [16], the authors expanded the work of [15] into a mobile-to-mobile (M2M) channel model, in which both the transmitter and the receiver can change their velocities over time. The temporal ACF and the Wigner spectrum of the proposed model were derived. The authors in [17] proposed a 2-D non-stationary channel model using a sum-of-chirps ( $SOC_h$ ) process and the Doppler PSD was analyzed through the Wigner spectrum. However, channel models in [15]–[17] are 2-D channel models and ignored the time evolution of clusters. Besides, the channel models in [15] and [16] can only model isotropic scattering environment.

In this paper, a 3-D non-stationary wideband MIMO channel model is proposed. The MS of the proposed channel model is allowed to move with an acceleration and move in curves, e.g., a sine shaped trajectory. The spatial CCF, temporal ACF, and Doppler PSD of the proposed channel model are derived and analyzed. It is shown that the motion of the MS has a significant impact on the statistical properties of the channel model. Furthermore, the channel model can be adapted to various scenarios by setting different channel parameters.

The remainder of this paper is organized as follows. In Section II, a 3-D non-stationary wideband MIMO channel

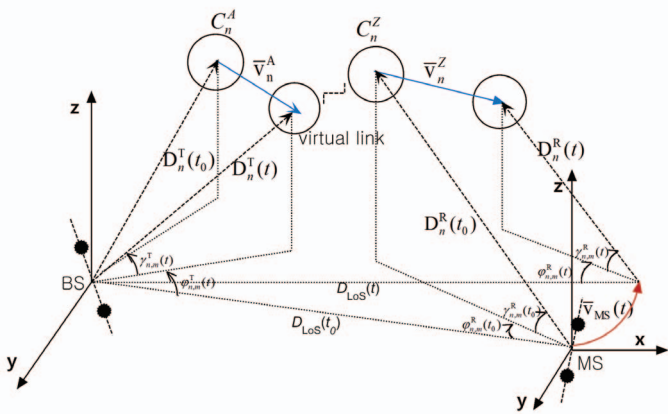


Fig. 1. BS and MS angular parameters in 3-D non-stationary channel model.

model is introduced. Statistical properties of the proposed channel model are studied in Section III. In Section IV, numerical and simulation results are presented and analyzed. Finally, the conclusions are drawn in Section V.

## II. A 3-D NON-STATIONARY WIDEBAND MIMO CHANNEL MODEL

Let us consider a 3-D propagation environment as illustrated in Fig. 1. We assume that the base station (BS) is fixed and the MS is allowed to travel along different trajectories with a constant acceleration in the X-Y plane. The velocity of the MS is presented by a vector  $\bar{v}_{\text{MS}}(t)$  with speed  $v_{\text{MS}}(t)$  and direction of motion  $\theta_{\text{MS}}(t)$ . Both terminals are equipped with uniform linear array (ULA) with omnidirectional antennas. The antenna array orientation of MS changes when MS move in curves, which results in a significant impact on the statistical properties of the channel model and we will discuss it in the rest of this paper. As shown in Fig. 1, the clusters disperse in a 3-D space and each cluster is composed of several rays which have similar angle parameters and the same delays. Considering a multi-bounce scattering propagation, a full propagation path consists of the first bounce propagation represented by  $C_n^A$  at BS side, the last bounce propagation represented by  $C_n^Z$  at the MS side, and the virtual link between them. The velocity vectors of  $C_n^A$  and  $C_n^Z$  are denoted by  $\bar{v}_n^A$  and  $\bar{v}_n^Z$ , respectively. The clusters are allowed to move with a certain probability  $P_c$  at random speeds. The key parameters involved in the channel model are listed in Table I.

### A. Channel Impulse Response

The channel coefficients in the non-line-of-sight (NLoS) case for the  $n$ -th cluster (consisting  $M$  rays) from transmit antenna element  $s$  ( $s = 1, 2, \dots, M_T$ ) to receive antenna element  $u$  ( $u = 1, 2, \dots, M_R$ ) can be expressed as [12]

$$h_{u,s,n}(t) = \sqrt{\frac{P_n(t)}{M}} \sum_{m=1}^M e^{j k \bar{r}_s \cdot \bar{\Phi}_{n,m}(t)} \cdot e^{j k \bar{r}_u(t) \cdot \bar{\Psi}_{n,m}(t)} \cdot e^{j 2\pi \nu_{n,m}(t) \cdot t} \cdot e^{j \Theta_{n,m}} \quad (1)$$

where  $k = 2\pi/\lambda$  is the free-space wave number and  $\lambda$  is the wavelength.  $P_n(t)$  is the time-variant power of the  $n$ -th path.  $\Theta_{n,m}$  is random initial phase which is uniformly distributed over the interval  $[0, 2\pi]$ .  $\bar{\Phi}_{n,m}(t)$  is the departure angle unit vector with elevation angles of departure (EAoD)  $\gamma_{n,m}^T(t)$  and azimuth angles of departure (AAoD)  $\varphi_{n,m}^T(t)$ , which can be expressed as

$$\bar{\Phi}_{n,m}(t) = \begin{bmatrix} \cos \gamma_{n,m}^T(t) \cdot \cos \varphi_{n,m}^T(t) \\ \cos \gamma_{n,m}^T(t) \cdot \sin \varphi_{n,m}^T(t) \\ \sin \gamma_{n,m}^T(t) \end{bmatrix}^T. \quad (2)$$

$\bar{\Psi}_{n,m}(t)$  is the arrival angle unit vector with elevation angles of arrival (EAoA)  $\gamma_{n,m}^R(t)$  and azimuth angles of arrival (AAoA)  $\varphi_{n,m}^R(t)$ , which is given by

$$\bar{\Psi}_{n,m}(t) = \begin{bmatrix} \cos \gamma_{n,m}^R(t) \cdot \cos \varphi_{n,m}^R(t) \\ \cos \gamma_{n,m}^R(t) \cdot \sin \varphi_{n,m}^R(t) \\ \sin \gamma_{n,m}^R(t) \end{bmatrix}^T. \quad (3)$$

$\bar{r}_s$  is the  $s$ -th transmit antenna vector with the elevation angle of the transmit antenna array  $\phi_E^T$  and the azimuth angle of the transmit antenna array  $\phi_A^T$ , that can be expressed as

$$\bar{r}_s = \frac{M_T - 2s + 1}{2} \delta_T \begin{bmatrix} \cos \phi_E^T \cdot \cos \phi_A^T \\ \cos \phi_E^T \cdot \sin \phi_A^T \\ \sin \phi_E^T \end{bmatrix}^T \quad (4)$$

where  $\delta_T$  is the distance between transmit antenna elements. Considering the speed and trajectory variations of the MS, the  $u$ -th receive antenna vector  $\bar{r}_u(t)$  is time-varying, and can be expressed as

$$\bar{r}_u(t) = \frac{M_R - 2u + 1}{2} \delta_R \begin{bmatrix} \cos \phi_E^R(t) \cdot \cos \phi_A^R(t) \\ \cos \phi_E^R(t) \cdot \sin \phi_A^R(t) \\ \sin \phi_E^R(t) \end{bmatrix}^T \quad (5)$$

where  $\delta_R$  is the distance between receive antenna elements,  $\phi_E^R(t)$  is the elevation angle of the arrival antenna array,  $\phi_A^R(t)$  is the azimuth angle of the transmit antenna array. The MS movement denoted by the MS velocity vector  $\bar{v}_{\text{MS}}(t)$  can be expressed as

$$\bar{v}_{\text{MS}}(t) = v_{\text{MS}}(t) \cdot \begin{bmatrix} \cos \vartheta_{\text{MS}}(t) \cdot \cos \theta_{\text{MS}}(t) \\ \cos \vartheta_{\text{MS}}(t) \cdot \sin \theta_{\text{MS}}(t) \\ \sin \vartheta_{\text{MS}}(t) \end{bmatrix}^T \quad (6)$$

where  $v_{\text{MS}}(t)$  is the speed of the MS,  $\vartheta_{\text{MS}}(t)$  is the travel elevation angle,  $\theta_{\text{MS}}(t)$  is the travel azimuth angle. We assume that the MS moves in the horizontal plane. The speed and angle of motion can be expressed as

$$v_{\text{MS}}(t) = v_0 + a \cdot t \quad (7)$$

$$\theta_{\text{MS}}(t) = \theta_0 + \omega \cdot t \quad (8)$$

where  $v_0$  is the initial velocity,  $a$  is the acceleration,  $\theta_0$  is the initial angle of motion, and  $\omega$  is the angular speed. The Doppler frequency component  $\nu_{n,m}(t)$  can be expressed as

$$\nu_{n,m}(t) = \frac{\bar{v}_{\text{MS}}(t) \cdot \bar{\Psi}_{n,m}(t)}{\lambda}. \quad (9)$$

TABLE I  
SUMMARY OF KEY PARAMETER DEFINITIONS.

$C_n^A$	the first bounce cluster of the $n$ -th path
$C_n^Z$	the last bounce cluster of the $n$ -th path
$\bar{D}_n^T(t)$	distance vector between BS and $C_n^A$
$\bar{D}_n^R(t)$	distance vector between MS and $C_n^Z$
$\bar{D}_{n,m}^T(t)$	distance vector between BS and $C_n^A$ via the $m$ -th ray
$\bar{D}_{n,m}^R(t)$	distance vector between MS and $C_n^Z$ via the $m$ -th ray
$D_{\text{LoS}}(t)$	distance of the LoS component between BS and MS
$\varphi_{n,m}^T(t), \varphi_{n,m}^R(t)$	azimuth angles of the $m$ -th ray of the $n$ -th path at the BS and the MS sides
$\gamma_{n,m}^T(t), \gamma_{n,m}^R(t)$	elevation angles of the $m$ -th ray of the $n$ -th path at the BS and the MS sides
$\bar{v}_n^A(t), \bar{v}_n^Z(t), \bar{v}_{\text{MS}}(t)$	velocity vectors of $C_n^A, C_n^Z$ , and MS
$v_n^A(t), \theta_n^A(t), \vartheta_n^A(t)$	speed, travel azimuth angle, and travel elevation angle of $C_n^A$
$v_n^Z(t), \theta_n^Z(t), \vartheta_n^Z(t)$	speed, travel azimuth angle, and travel elevation angle of $C_n^Z$
$v_{\text{MS}}(t), \theta_{\text{MS}}(t), \vartheta_{\text{MS}}(t)$	speed, travel azimuth angle, and travel elevation angle of MS
$\phi_A^T(t), \phi_A^R(t)$	azimuth angles of the transmit and receive antenna arrays
$\phi_E^T(t), \phi_E^R(t)$	elevation angles of the transmit and receive antenna arrays

### B. Cluster Time Evolution

The non-stationarity of the channel model is represented by the cluster time evolution and the time-variant parameters. We use a birth-death process to simulate the generation-recombination behavior of clusters. For the newly born clusters, the parameters of clusters such as delays, powers, and angles are generated similar to the initial parameters. For the surviving clusters, the parameters of clusters are updated according to the geometrical relationships among clusters, transmitter, and receiver, which will be introduced in the rest of this subsection.

1) *Birth-death process*: In the non-stationary scenario, the clusters only exist over a certain time period. A birth-death process [18] is adopted to model the clusters' appearance and disappearance. The time dependent channel fluctuations caused by the movement of scatterers, i.e.,  $\delta_{\text{MC},n}(t, \Delta t)$  and the movement of MS, i.e.,  $\delta_{\text{MS}}(t, \Delta t)$  in the time span between  $t$  and  $t + \Delta t$  can be expressed as

$$\delta_P(t, \Delta t) = \delta_{\text{MC},n}(t, \Delta t) + \delta_{\text{MS}}(t, \Delta t) \quad (10)$$

with

$$\delta_{\text{MC},n}(t, \Delta t) = \int_t^{t+\Delta t} P_c \cdot (|\bar{v}_n^A(t)| + |\bar{v}_n^Z(t)|) dt \quad (11)$$

and

$$\delta_{\text{MS}}(t, \Delta t) = \int_t^{t+\Delta t} (|\bar{v}_{\text{MS}}(t)|) dt \quad (12)$$

where  $P_c$  is the probability of clusters movement. The mean velocities of clusters, i.e.,  $v^A = E[v_n^A]$  and  $v^Z = E[v_n^Z]$  are used in this birth-death process and considering the time-variant velocity of the MS, (11) and (12) can be rewritten as

$$\delta_{\text{MC}}(\Delta t) = P_c \cdot (v^A + v^Z) \cdot \Delta t \quad (13)$$

and

$$\delta_{\text{MS}}(t, \Delta t) = (v_0 + a \cdot t) \cdot \Delta t. \quad (14)$$

The clusters in time instant  $t + \Delta t$  can be assumed as the sum of the surviving clusters from time instant  $t$  and the newly

born clusters during the time interval  $\Delta t$ . The birth-death process is controlled by the generation rate of clusters  $\lambda_G$  and the recombination rate of clusters  $\lambda_R$ . The initial number of clusters in the proposed channel model is given by

$$E[N(t)] = \frac{\lambda_G}{\lambda_R}. \quad (15)$$

The probabilities of clusters at  $t + \Delta t$  survived from  $t$  can be modeled as

$$P_{\text{survival}}(t, \Delta t) = e^{-\lambda_R \cdot \frac{\delta_P(t, \Delta t)}{D_c}} \quad (16)$$

where  $D_c$  is the scenario dependent correlation factor. The expectation of the number of newly generated clusters can be calculated as

$$E[N_{\text{new}}(t + \Delta t)] = \frac{\lambda_G}{\lambda_R} (1 - e^{-\lambda_R \cdot \frac{\delta_P(t, \Delta t)}{D_c}}). \quad (17)$$

2) *Evolution of surviving clusters*: For the surviving clusters, the parameters are updated based on the geometrical relationships from  $t$  to  $t + \Delta t$ . The position vector from BS to the  $C_n^A$ , i.e.,  $\bar{D}_n^T(t)$  and position vector from MS to the  $C_n^Z$ , i.e.,  $\bar{D}_n^R(t)$  can be expressed as

$$\bar{D}_n^T(t) = \bar{D}_n^T(t_0) + \bar{v}_n^A \cdot t \quad (18)$$

and

$$\bar{D}_n^R(t) = \bar{D}_n^R(t_0) + \bar{v}_n^Z \cdot t - \bar{v}_{\text{MS}} \cdot t. \quad (19)$$

The position vector from BS to the  $C_n^A$  via the  $m$ -th ray which is denoted by  $\bar{D}_{n,m}^T(t)$  and position vector from MS to the  $C_n^Z$  via the  $m$ -th ray which is denoted by  $\bar{D}_{n,m}^R(t)$  can be calculated as

$$\bar{D}_{n,m}^T(t) = \bar{D}_{n,m}^T(t_0) + \bar{v}_n^A \cdot t \quad (20)$$

and

$$\bar{D}_{n,m}^R(t) = \bar{D}_{n,m}^R(t_0) + \bar{v}_n^Z \cdot t - \bar{v}_{\text{MS}} \cdot t. \quad (21)$$

The initial distance  $\bar{D}_{n,m}^T(t_0)$  and  $\bar{D}_{n,m}^R(t_0)$  are assumed to follow a Gaussian distribution, i.e.,  $D_{n,m}^T(t_0) \sim$

$N(D_n^T(t_0), \sigma_D)$  and  $D_{n,m}^R(t_0) \sim N(D_n^R(t_0), \sigma_D)$ , where  $\sigma_D$  is the cluster spread depends on specific scenarios. The delay of the  $n$ -th path at time  $t$  can be calculated as

$$\tau_n(t) = \frac{|D_n^T(t)| + |D_n^R(t)|}{c} + \tilde{\tau}_n(t) \quad (22)$$

where  $\tilde{\tau}(t)$  is the delay of the virtual link between  $C_n^A$  and  $C_n^Z$ , which is calculated based on a first-order filtering algorithm [8]  $\tilde{\tau}_n(t) = e^{-\frac{\Delta t}{\zeta}} \cdot \tilde{\tau}_n(t - \Delta t) + (1 - e^{-\frac{\Delta t}{\zeta}}) \cdot X$ , where  $X \sim U(D_{\text{LoS}}(t)/c, \tau_{\max})$ . The angular parameters are obtained from the position vectors  $\bar{D}_{n,m}^T(t)$  and  $\bar{D}_{n,m}^R(t)$  by transforming the Cartesian coordinates into polar coordinates.

### III. STATISTICAL PROPERTIES

#### A. Spatial-Temporal Correlation Function

The spatial-temporal correlation function between the channel coefficients  $h_{u_1,s_1,n}$  and  $h_{u_2,s_2,n}$  is defined as [19]

$$\rho_{s_2,u_2,n}^{s_1,u_1}(t, \Delta t, \delta_T, \delta_R) = E \left\{ \frac{h_{u_1,s_1,n}^*(t) \cdot h_{u_2,s_2,n}(t + \Delta t)}{|h_{u_1,s_1,n}^*(t)| \cdot |h_{u_2,s_2,n}(t + \Delta t)|} \right\} \quad (23)$$

where  $(\cdot)^*$  denotes the complex conjugation operation. By substituting (1) into (23), the spatial-temporal correlation function can be calculated as

$$\begin{aligned} \rho_{s_2,u_2,n}^{s_1,u_1}(t, \Delta t, \delta_T, \delta_R) &= \frac{1}{M} \sum_{m=1}^M e^{jk[\bar{r}_{s_2} \cdot \bar{\Phi}_{n,m}(t + \Delta t) - \bar{r}_{s_1} \cdot \bar{\Phi}_{n,m}(t)]} \\ &\quad \cdot e^{jk[\bar{r}_{u_2}(t + \Delta t) \cdot \bar{\Psi}_{n,m}(t + \Delta t) - \bar{r}_{u_1}(t) \cdot \bar{\Psi}_{n,m}(t)]} \\ &\quad \cdot e^{j2\pi[\nu_{n,m}(t + \Delta t) \cdot (t + \Delta t) - \nu_{n,m}(t) \cdot t]}. \end{aligned} \quad (24)$$

#### B. Spatial Cross-Correlation Function

By imposing  $\Delta t = 0$  in (24), we get the spatial CCF between  $h_{u_1,s_1,n}$  and  $h_{u_2,s_2,n}$ , which can be expressed as

$$\begin{aligned} \rho_{s_2,u_2,n}^{s_1,u_1}(t, \delta_T, \delta_R) &= \frac{1}{M} \sum_{m=1}^M e^{jk \cdot (\bar{r}_{s_2} - \bar{r}_{s_1}) \cdot \bar{\Phi}_{n,m}(t)} \\ &\quad \cdot e^{jk \cdot [\bar{r}_{u_2}(t) - \bar{r}_{u_1}(t)] \cdot \bar{\Psi}_{n,m}(t)}. \end{aligned} \quad (25)$$

If we let  $\delta_T = 0$ , i.e., two links share the same transmit antenna element, we obtain the spatial CCF observed at MS, which can be expressed as

$$\rho_{u_1,u_2,n}^{\text{MS}}(t, \delta_R) = \frac{1}{M} \sum_{m=1}^M e^{jk \cdot [\bar{r}_{u_2}(t) - \bar{r}_{u_1}(t)] \cdot \bar{\Psi}_{n,m}(t)}. \quad (26)$$

#### C. Temporal Autocorrelation Function

The temporal ACF can be obtained by imposing  $\delta_T = 0$  and  $\delta_R = 0$  in (24), which can be expressed as

$$\begin{aligned} \rho_{s_1,u_1,n}(t, \Delta t) &= P_{\text{survival}} \\ &\quad \cdot \frac{1}{M} \sum_{m=1}^M e^{j2\pi[\nu_{n,m}(t + \Delta t) \cdot (t + \Delta t) - \nu_{n,m}(t) \cdot t]} \end{aligned} \quad (27)$$

where  $P_{\text{survival}} = e^{-\frac{\lambda_R}{D_c} \cdot [(v_0 + a \cdot t) \cdot \Delta t + P_c \cdot (v^A + v^Z) \cdot \Delta t]}$ , which means a cluster has a probability of  $P_{\text{survival}}$  to survive from  $t$  to  $t + \Delta t$ .

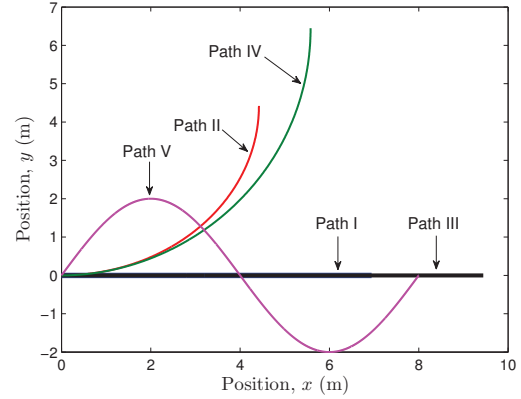


Fig. 2. Different trajectories of MS.

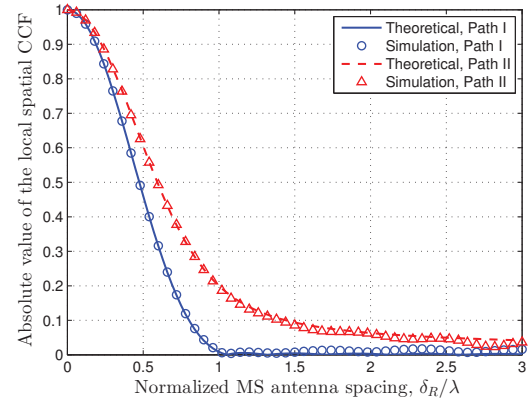


Fig. 3. The theoretical and simulation spatial CCFs of the proposed channel model at different angular speeds (UMi NLoS scenario,  $t = 2$  s,  $\varphi_1^R(t_0) = 0$ ,  $v_{\text{MS}}(t_0) = 5$  km/h,  $a = 0$  m/s $^2$ ,  $\theta_{\text{MS}}(t_0) = 0$ ,  $v_n^A$  and  $v_n^Z \sim U(0, 5)$  m/s,  $\theta_n^A$  and  $\theta_n^Z \sim U(-\pi, \pi)$ ,  $\vartheta_n^A$  and  $\vartheta_n^Z \sim U(-\pi/2, \pi/2)$ ).

#### D. Doppler Power Spectral Density

The Doppler PSD  $S_n(f, t)$  of the proposed channel model is obtained by the Fourier transform of the temporal ACF  $\rho_{s_1,u_1,n}(t, \Delta t)$  with respect to the time interval  $\Delta t$ , which can be expressed as

$$S_n(f, t) = \int_{-\infty}^{\infty} \rho_{s_1,u_1,n}(t, \Delta t) \cdot e^{-j2\pi f \Delta t} d(\Delta t). \quad (28)$$

### IV. RESULTS AND ANALYSIS

As shown in Fig. 2, five typical paths are selected for studying the impact on the statistical properties caused by the velocity variations, the parameters of which are listed as follows: path I,  $a = 0$  m/s $^2$ ,  $\omega = 0$  s $^{-1}$ , path II,  $a = 0$  m/s $^2$ ,  $\omega = \pi/10$  s $^{-1}$ , path III,  $a = 0.2$  m/s $^2$ ,  $\omega = 0$  s $^{-1}$ , path IV,  $a = 0.2$  m/s $^2$ ,  $\omega = \pi/10$  s $^{-1}$ . Other parameters are the same to the four paths, i.e.,  $v_0 = 5$  km/h,  $\theta_0 = 0$ . For the last path, the MS moves along a sine routine, i.e.,  $y = 2\sin(\frac{\pi x}{4})$  with an acceleration  $a = 0.2$  m/s $^2$ . The theoretical and simulation spatial CCFs of the proposed channel model for path I and path II are shown in Fig. 3. It can be observed that the increase

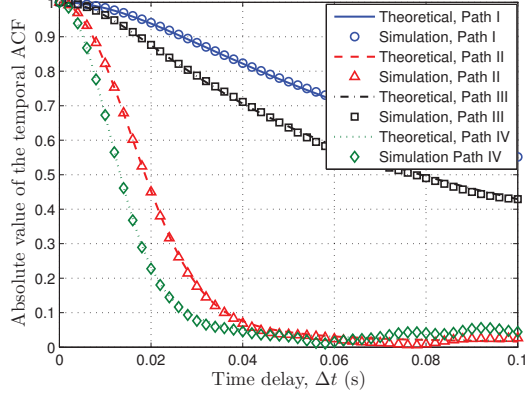


Fig. 4. The theoretical and simulation temporal ACFs of the proposed channel model at different angular speeds and accelerations (UMi NLoS scenario,  $t = 2$  s,  $v_{\text{MS}}(t_0) = 5$  km/h,  $\varphi_1^R(t_0) = 0$ ,  $\theta_{\text{MS}}(t_0) = 0$ ,  $v_n^A$  and  $v_n^Z \sim U(0, 5)$  m/s,  $\theta_n^A$  and  $\theta_n^Z \sim U(-\pi, \pi)$ ,  $\vartheta_n^A$  and  $\vartheta_n^Z \sim U(-\pi/2, \pi/2)$ ).

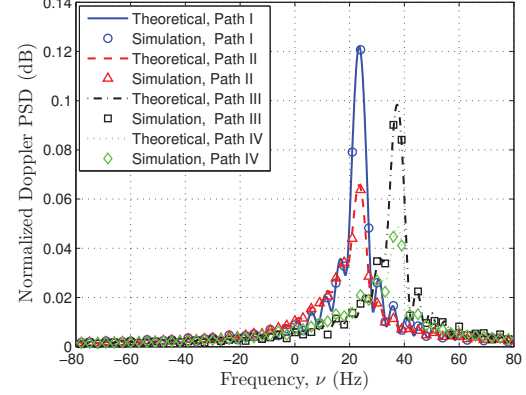


Fig. 5. The theoretical and simulation normalized Doppler PSDs of the proposed channel model at different angular speeds and accelerations (UMi NLoS scenario,  $t = 2$  s,  $\varphi_1^R(t_0) = 0$ ,  $v_{\text{MS}}(t_0) = 5$  km/h,  $\theta_{\text{MS}}(t_0) = 0$ ,  $v_n^A$  and  $v_n^Z \sim U(0, 5)$  m/s,  $\theta_n^A$  and  $\theta_n^Z \sim U(-\pi, \pi)$ ,  $\vartheta_n^A$  and  $\vartheta_n^Z \sim U(-\pi/2, \pi/2)$ ).

in the angles between direction of incident wave and the direction of motion of the MS results in strong receive antenna correlations. Besides, (25) indicates that the acceleration has no effect on the spatial CCFs of the channel. The theoretical and simulation temporal ACFs of the proposed channel model for path I-IV are illustrated in Fig. 4. Contrary to the situation in spatial CCFs, the larger angles between direction of incident wave and the direction of motion of the MS, the weaker time autocorrelations of the channel impulse responses (CIRs) can be observed. Furthermore, the temporal ACFs decrease faster when the MS with an acceleration, i.e., the faster the MS moves, the weaker the autocorrelations of CIRs over time. Fig. 5 shows the the theoretical and simulation normalized Doppler PSDs of the proposed channel model for path I-IV. The channel has a larger doppler frequency shift when the MS with an acceleration, which is consistent with the theoretical analysis. Meanwhile, the movement direction of MS has an effect on the distributions of Doppler PSDs, i.e., the Doppler PSDs are more concentrated when the angles between the movement direction of MS and the direction of incident wave are smaller. Figs. 6–8 are simulated where the MS moves along a sine curve with an initial speed of 5 km/h and an acceleration of  $0.2 \text{ m/s}^2$ . Fig. 6 and Fig. 7 show the time-variant spatial CCFs and time-variant temporal ACFs of the proposed channel model. The variations of movement directions of the MS causing a great impact on the statistical properties of the channel model can be observed, i.e., the movement directions of the MS have opposite effects on temporal and spatial correlations. Fig. 8 illustrates the time-variant Doppler PSDs of the proposed channel model. The Doppler PSDs change regularly with the trajectory of the MS. The peak of the Doppler PSDs shift to larger values as the speed of the MS increases. Besides, the distributions of the Doppler PSDs are most concentrated when the MS moves to the locations of extreme values of the sine curve.

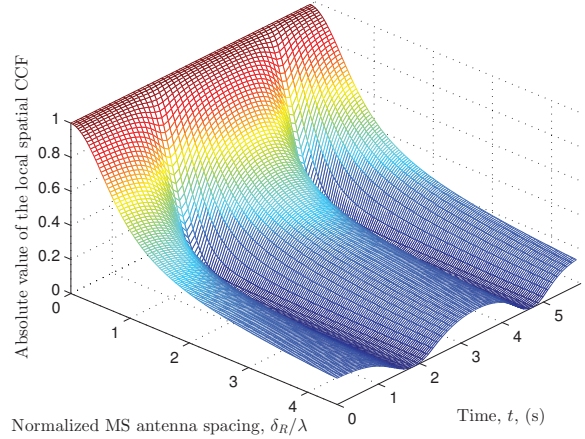


Fig. 6. The spatial CCFs of the proposed channel model for path V (UMi NLoS scenario,  $\varphi_1^R(t_0) = 0$ ,  $v_{\text{MS}}(t_0) = 5$  km/h,  $a = 0.2 \text{ m/s}^2$ ,  $v_n^A$  and  $v_n^Z \sim U(0, 5)$  m/s,  $\theta_n^A$  and  $\theta_n^Z \sim U(-\pi, \pi)$ ,  $\vartheta_n^A$  and  $\vartheta_n^Z \sim U(-\pi/2, \pi/2)$ ).

## V. CONCLUSIONS

In this paper, a 3-D non-stationary wideband MIMO channel model has been proposed. The speed and movement direction of the MS are allowed to change over time. The cluster time evolution is modeled using a birth-death process. The parameters including delays, powers, angles of departure, and angles of arrival are updated based on the geometric construction of the channel model. Statistical properties including spatial CCF, temporal ACF, and Doppler PSD have been investigated. The results show that the MS at different speeds and/or with different movement directions can cause significant influences on the statistics of the channel model. Furthermore, the simulation results match the theoretical results very well, verifying the correctness of our derivations and simulations.

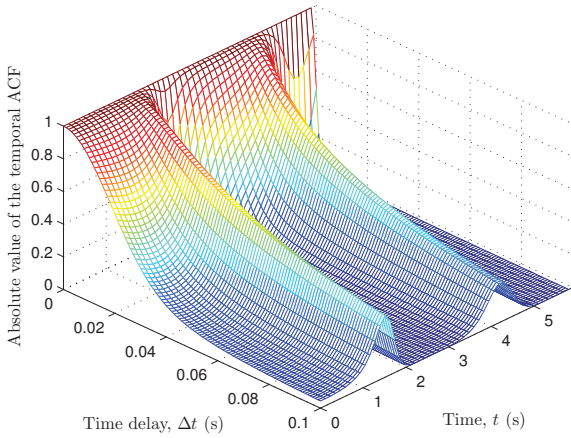


Fig. 7. The temporal ACFs of the proposed channel model for path V (UMi NLoS scenario,  $\varphi_1^R(t_0) = 0$ ,  $v_{\text{MS}}(t_0) = 5 \text{ km/h}$ ,  $a = 0.2 \text{ m/s}^2$ ,  $v_n^A$  and  $v_n^Z \sim U(0, 5) \text{ m/s}$ ,  $\theta_n^A$  and  $\theta_n^Z \sim U(-\pi, \pi)$ ,  $\vartheta_n^A$  and  $\vartheta_n^Z \sim U(-\pi/2, \pi/2)$ ).

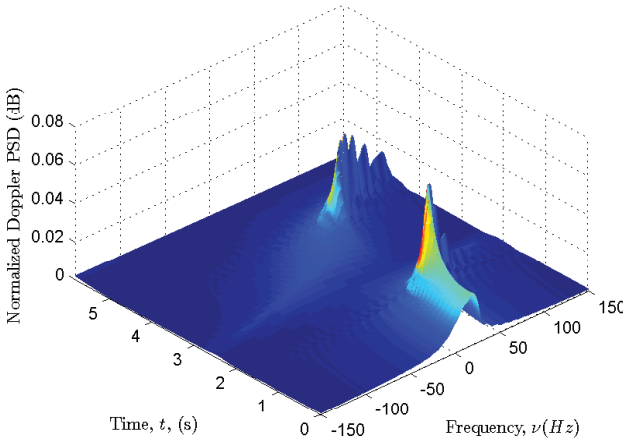


Fig. 8. The Doppler PSDs of the proposed channel model for path V (UMi NLoS scenario,  $\varphi_1^R(t_0) = 0$ ,  $v_{\text{MS}}(t_0) = 5 \text{ km/h}$ ,  $a = 0.2 \text{ m/s}^2$ ,  $v_n^A$  and  $v_n^Z \sim U(0, 5) \text{ m/s}$ ,  $\theta_n^A$  and  $\theta_n^Z \sim U(-\pi, \pi)$ ,  $\vartheta_n^A$  and  $\vartheta_n^Z \sim U(-\pi/2, \pi/2)$ ).

#### ACKNOWLEDGEMENT

The authors gratefully acknowledge the support from the EPSRC TOUCAN project (Grant No. EP/L020009/1), the EU FP7 QUICK project (Grant No. PIRSES-GA-2013-612652), the EU H2020 5G Wireless project (Grant NO. 641985), Natural Science Foundation of China (Grant No. 61210002 and 61371110), and Key R&D Program of Shandong Province (Grant No. 2016GGX101014).

#### REFERENCES

- [1] C.-X. Wang, F. Haider, X. Q. Gao, X.-H. You, Y. Yang, D. Yuan, H. Aggoune, H. Haas, S. Fletcher, and E. Hepsaydir, "Cellular architecture and key technologies for 5G wireless communication networks," *IEEE Commun. Mag.*, vol. 52, no. 2, pp. 122–130, Feb. 2014.
- [2] METIS, "Scenarios, requirements and KPIs for 5G mobile and wireless system," [http://publications.lib.chalmers.se/records/fulltext/213055/local\\_213055.pdf](http://publications.lib.chalmers.se/records/fulltext/213055/local_213055.pdf).
- [3] I. Gaspar and G. Wunder, "5G cellular communications scenarios and system requirements," <http://is-wireless.com/fp7-5gnow/5gnow-deliverables-5g-cellular-communications-scenarios-and-system-requirements/>.
- [4] Huawei, 5G a technology vision. White Paper. [https://www.huawei.com/-/link/en/download/HW\\_314849](https://www.huawei.com/-/link/en/download/HW_314849).
- [5] B. Chen, Z. Zhong, and B. Ai, "Stationarity intervals of time-variant channel in high speed railway scenario," *J. China Commun.*, vol. 9, no. 8, pp. 64–70, Aug. 2012.
- [6] M. V. S. N. Prasad, K. Ratnamla, and P. K. Dalela, "Mobile communication measurements along railroads and model evaluations over eastern-indian rural regions," *IEEE Antennas Propag. Mag.*, vol. 52, no. 5, pp. 131–141, Oct. 2010.
- [7] L. Liu, C. Tao, J. Qiu, H. Chen, L. Yu, W. Dong, and Y. Yuan, "Position-based modeling for wireless channel on high-speed railway under a viaduct at 2.35 Ghz," *IEEE J. Sel. Areas Commun.*, vol. 30, no. 4, pp. 834–845, May 2012.
- [8] S. Wu, C.-X. Wang, e. H. M. Aggoune, M. M. Alwakeel, and Y. He, "A non-stationary 3-D wideband twin-cluster model for 5G massive MIMO channels," *IEEE J. Sel. Areas Commun.*, vol. 32, no. 6, pp. 1207–1218, Jun. 2014.
- [9] L. Liu, C. Oestges, J. Poutanen, K. Haneda, P. Vainikainen, F. Quitin, F. Tufvesson, and P. D. Doncker, "The COST 2100 MIMO channel model," *IEEE Wireless Commun. Mag.*, vol. 19, no. 6, pp. 92–99, Dec. 2012.
- [10] 3GPP TR 25.996 v13.1.0, "Spatial channel model for multiple input multiple output simulations," Release 13, Dec. 2016.
- [11] P. Kyösti, et al., "WINNER II channel models," IST-4-027756, WINNER II D1.1.2, v1.2, Apr. 2008.
- [12] J. Meinila, P. Kyösti, L. Hentila, T. Jamsa, E. Suikkanen, E. Kunnari, and M. Narandzia, "D5.3: WINNER+ final channel models," CELTIC/CP5-026, Jun. 2010.
- [13] 3GPP TR 36.873, V12.0.0, "3rd generation partnership project, technical specification group radio access network, study on 3D channel model for LTE (Release 12)," Jun. 2015.
- [14] R. Iqbal and T. D. Abhayapala, "Impact of mobile acceleration on the statistics of rayleigh fading channel," in *Proc. AusCTW'07*, Adelaide, Australia, May 2015, pp. 1–4.
- [15] M. Pätzold and A. Borhani, "A non-stationary multipath fading channel model incorporating the effect of velocity variations of the mobile station," in *Proc. WCNC'14*, Istanbul, Turkey, Apr. 2014, pp. 182–187.
- [16] W. Dahech, M. Pätzold, and N. Youssef, "A non-stationary mobile-to-mobile multipath fading channel model taking account of velocity variations of the mobile stations," in *Proc. EuCAP 2015*, Lisbon, Portugal, May 2015, pp. 1–4.
- [17] M. Pätzold and C. A. Gutierrez, "The Wigner distribution of sum-of-cissoids and sum-of-chirps processes for the modelling of stationary and non-stationary mobile channels," in *Proc. IEEE VTC'16-Spring*, Nanjing, China, May 2016, pp. 1–5.
- [18] T. Zwick, C. Fischer, D. Didascalou, and W. Wiesbeck, "A stochastic spatial channel model based on wave-propagation modeling," *IEEE J. Sel. Areas Commun.*, vol. 18, no. 1, pp. 6–15, Jan. 2000.
- [19] C.-X. Wang, X. Hong, H. Wu, and W. Xu, "Spatial-temporal correlation properties of the 3GPP spatial channel model and the kronecker MIMO channel model," *Eurasip J. Wireless Commun. Netw.*, vol. 2007, no. 1, pp. 39 817-1–39 817-9, Feb. 2007.